Studies of Structural and Magnetic Properties of $NiFe_2O_4$ by Low Temperature Neutron Diffraction Experiments

I.B. Elius[1*], S. Saha[2], T.K. Datta[1], S. Hossain[1*], J. Maudood[1], M.S. Aktar[1], I. Kamal[3]
A.K. M Zakaria[3], S.M. Yunus[3] and K.A. Kabir[4]

[1]*Institute of Nuclear Science and Technology, Bangladesh Atomic Energy Commission*
G P O Box No. 3787, Dhaka-1000, Bangladesh
[2]*Nuclear Power and Energy Division, Agargaon, Sher-e-Bangla Nagar, Dhaka-1207*
[3]*Bangladesh Atomic Energy Commission, Agargaon, Sher-e-Bangla Nagar, Dhaka-1207*
[4]*Department of Nuclear Engineering, University of Dhaka, Dhaka-1000*

Abstract

The nickel doped spinel ferrite ($NiFe_2O_4$) was synthesized via PVA evaporation method. The powder sample of the material was subjected to neutron diffraction studies to determine its structural as well as magnetic properties. To observe the effect of its crystalline and magnetic structureinlow temperature the neutron diffraction experiments were carried out at 298K, 200K, 100K, 50K and 10K. The experimental data were analyzed by Rietveld refinement method. It was found that the material belonged to Fd-3m space group, cell parameter reduces from 8.3028Å at 298K to 8.2896Å at 10K. The gradual change of structural parameters, distances and angles of interaction of the anions and cations, bond lengths, interaction angles were observed with the variation of temperatures. The magnetic moment of the material was also determined from the analyzed data.

Keywards: Neutron diffraction, Ferrites, Rietveld refinement, Magnetic materials, PVA evapotaion method

1. Introduction

Spinel or to be specific, spinel ferrites are at the centers of various studies in materials science and solid-state physics because of their intriguing magnetic properties. Primarily they have various uses as inductive components in low noise amplifiers, voltage-controlled oscillators, magnetic field sensors, electromagnetic interface suppression etc. In recent years, the attention has been intensified because of their applicability in bio and medical physics as site specific drug delivery, magnetic storage system, photo-magnetic materials, water treatment, gas sensors etc. [1, 2].The neutron scattering is a unique experiment that gives an atomic-level view of magnetic interactions. In spinel ferrites the interplay between two sub-lattices, inter and the intra tetrahedral and octahedral interactions mediate the magnetic characteristic of the crystal. The magnetic properties of the spinel ferrites can be engineered or altered depending on the dopant, amount of doping, sintering temperatures, process of synthesis etc. Neel's model for ferromagnetic materials can successfully explain the magnetic characteristics of spinels having one or more magnetic cations. This is done by assuming the tetra and octahedral contributions are perfectly co-linear.

The spinel ferrites have a common formula $AO.B_2O_3$ (more compactly AB_2O_4); where A is at the centre of the tetrahedral sublattice and B forms the octahedral sublattice, sharing the oxygen anions, they form a spinel super-cell. Such a supercell houses eight (8) tetrahedral sub-cells and sixteen (16) octahedral sub-cells, and in total thirty-two (32) oxygen positions. The interaction between the cations might be A-A (J_{AA}), B-B (J_{BB}) and A-B (J_{AB}), which are mediated by the anions. The divalent cations normally occupies the A-position and the trivalent cations occupy the B-positions, if the opposite happens the spinel system is then called 'inverse spinel', and in case the divalents and trivalents share the both positions, the system is called mixed spinels, where the extent of inversion is measured by a factor γ (where $0 \leq \gamma \leq 1$) [3]. Several software and formulae were used for studying the crystalline parameters, magnetic moments and sizes of cations, bond lengths and interaction angles etc. Some of these software are, FullProf which uses the Rietveld technique, VESTA and BondStr were used for structural simulation [4-6]. In this study, effect of low temperature on magnetic moment change was investigated. To find out any sudden altercation in magnetic moment due to temperature change, the temperature was varied from room temperature to 10K.

*Corresponding author: *iftakhar.elius@gmail.com*

2. Materials and Method

2.1 Sample preparation and purity check

Nickel ferrite ($NiFe_2O_4$) was prepared by PVA evaporation method at the Institute of Nuclear Science and Technology (INST) of Atomic Energy Research Establishment (AERE), Savar, Dhaka. The 1 mole of $Ni(NO_3)_2.6H_2O$ (98% pure) and 2 moles $Fe(NO_3)_3.9H_2O$ (98% pure) were the parent materials in exact stoichiometric proportions. Furthermore, 3 moles polyvinyl alcohol (PVA) was used with the above chemicals. The ingredients were weighed separately in precise amount using a digital micro-balance. At first, $Ni(NO_3)_2.6H_2O$ and $Fe(NO_3)_3.9H_2O$ were mixed with requisite amount of de-ionized water and PVA. The mixture was then heated in a magnetic heater until all of the water vaporized and turned into ashes. Then it was heated in a box furnace (temperature range up to 1500°C) in air atmosphere at 700°C for 3 hours. After that the mixture was cooled inside the same furnace in the same atmosphere. After that, the mixture was grinded in an agate mortar until the particles become slippery and great care was taken so

that sample could not get contaminated. Small amount of polyvinyl alcohol (PVA) was added again to the dried mixture as binder and was intimately mixed by agate mortar. It was then pressed into small discs shaped pellet each of 2 g under a hydraulic press of 13 mm diameter applying 5 tons of pressure. The pellets were then pre-sintered in air at 1000°C for 6 hours. After heating, the furnace was turned off to reduce the temperature. Then the pellets of the sample were converted into powder by agate mortar. Some polyvinyl alcohol (PVA) was added again to the sample as binder and was intimately mixed by agate mortar. It was then pressed into pellets by the same process and pressure.The main reason to use polyvinyl alcohol is to distribute cations in its polymeric network homogenously and also restrict the segregation via precipitation from the solution [7]. When heated, the PVA is decomposed and thus an oxidising environment is created. As the NO_2 is evaporated an fluffy dark precursor is yielded. After the calcination process, porous-fine white powder is yielded as the organic parts evaporate as CO_2, CO, water and other gas forms. The pellets were finally sintered in air at 1100°C for 6 hours. Then the pellets were converted into powder form again by grinding 3 hours in agate mortar for neutron diffraction experiment.We used the method for preparing the samples developed by P. pramanik et al. [8]. The phase purity of the material was studied by the neutron diffraction technique.

2.2 Neutron diffraction data collection and refinement

Neutron diffraction is a technique to investigate theatomic and magnetic structures of a material. To investigate the magnetic structure and the site specific moments, the nickel ferrite sample was subjected to neutron diffraction studies by a high resolution neutron powder diffractometer (HRNPD) at the 3MW TRIGA Mark-II reactor at AERE, Savar, Dhaka. This diffractometer is a powder diffractometer that was set at the radial beam port-II of the research reactor. It has an assembly of 15 element ^{3}He gas position sensitive neutron detectors; the assembly is maneuverable with a mechanical arm around the target or sample table. Each step spans a range of 20° and a total 2θ range of 5°-120°. Its spectral resolution is 0.05°. The white neutron beam emanating from the research reactor is filtered to a monochromatic beam of λ= 1.5656Å using a focusing monochromator placed between the beam port and sample. The monochromator here is an assembly of nine (09) doubly bent single crystal silicon (Si) slabs each having dimension of 0.570×0.210×7.50 cubic inches. The beam of λ= 1.5656Å is drawn from the Bragg's reflection of (*511*) which corresponds to a takeoff angle of 97°. A cylindrical vanadium can (height = 5 cm, radius = 0.3cm) was filled with approximately 6 gm of nickel ferrite sample in powder form for neutron diffraction studies [9, 10].

The low temperature environment was created using an Advanced Research System (ARS)'s cryogenic refrigerator system. The total system consists of a bi-layer vacuum shroud, radiant heat shield, sample holder, a Pfeiffer Hi-cube vacuum station etc. This dual-stage device has two cold copper flanges. The top flange anchors an aluminum heat shield that surrounds the second stage cold finger and neutron diffraction outer sample can. The Pfeiffer Hi-Cube vacuum station combines a diaphragm pump with a turbomolecular pump to provide a compact and efficient system for evacuating the high temperature furnace and cryorefrigerator sample environments [9].

Two Si diode sensors are attached to the cold finger and sample. The upper sensor is attached just above the copper tip and is used to control the power to the heater, allowing operation up to room temperature. The lower sensor is attached to the bottom of the outer sample can, allowing the true sample temperature to be estimated as the mean value between these two readings. The outer sample can is sealed with an indium O-ring, and must be backfilled with He gas to provide good thermal contact over the length of the sample. The ARS cold head is attached to the custom built vacuum jacket by an O-ring in the square flange immediate below it. The head contains 3 ports; two are for supply and return of the high pressure He gas. This is delivered through 12' armored hoses. The connection between hoses and cold head are color coded, red for supply and green for return. The third access is for electrical power to the cold head, which is supplied from a connector labeled "expander power" on the compressor unit. The total system is driven by a Lakeshore controller. After performing neutron diffraction experiment at ambient temperature of 298K with the Lakeshore controller the sample temperature was set at 200K, 100K, 50K and finally 10K.

3. Results and Discussion

The neutron diffraction data were refined using the Rietveld based refinement program FullProf [4]. Often in the spinel ferrites, the crystalline and the magnetic structure is the same. The structural and the magnetic peaks coincide with each other. In that case, the magnetic contributions are dominant in the lower angle region [11]. To avoid the ambiguity arisen from the magnetic contributions, initially the cation distribution of the $NiFe_2O_4$ was determined using the diffraction data at higher Bragg's angle region ($50° \leq 2\theta \leq 110°$). Fig. 1 shows the neutron diffraction patterns of $NiFe_2O_4$ taken at temperature of 298K, 200K, 100K, 50K and 10K; respectively.

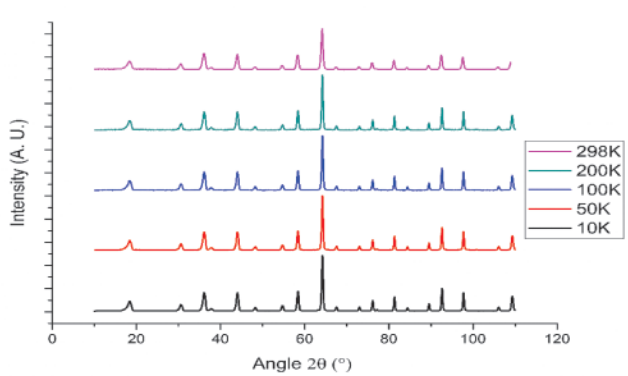

Fig. 1: Neutron diffraction patterns of $NiFe_2O_4$ performed at temperature of 298K, 200K, 100K, 50K and 10K, respectively

All the cations are magnetic (i.e. Ni^{2+}, Fe^{2+} and Fe^{3+}) and cubic spinel ferrites normally belong to space group Fd-3m. Initially the peaks were indexed and compared with the standard spinel ferrites diffraction pattern.The neutron diffraction data of the nickel ferrite sample were indexed using 'Chekcell' software. It indicates that all the patterns resemble the characteristic diffraction pattern of spinel ferrites having space group *Fd-3m*(O^7_h).No other unwanted peaks were observed which are indicative of unwanted phase or impurities.

The magnetic structure of the sample retains the parent groups structure and using the 'K-search' software, the propagation vector *k* was found to be (0, 0, 0) [12]. The background of the diffraction pattern was simulated with a six coefficient Chebyshev polynomial function, the peak shapes were fitted using Pseudo-Voigt function [11]. The overall pattern was fitted considering the structural and the magnetic as two different phases, the former as *Fd-3m* and the later as *F-1*. The peaks below 65° were corrected for asymmetry. The cell positions of the A site used were (0.125, 0.125, 0.125) and for B site position (0.5, 0.5, 0.5). Values of scattering lengths used for nickel was 1.030×10^{12} b_{coh}/cm, iron 0.9450×10^{12} b_{coh}/cm and for oxygen $0.5803\times10^{12}b_{coh}$/cm [13]. Cell parameters, position of the origin, first two factors of the Chebyshev polynomial were varied and refined initially. Then the oxygen position parameters, overall temperature factor andotherfactors such as, Chebyshev polynomial, asymmetry factor, FWHM parameters, shape parameters etc. were varied for a better fitting. Finally, the magnetic contributions from the magnetic cations were refined for the lowest possible values of the reliability factors. Eventually, in total of 16 different parameters were varied to refine the data [14]. Fig. 2 (a) shows the structure of $NiFe_2O_4$ super-cell (in which the golden spheres are tetrahedral (A), purple spheres indicate the octahedral ions (B), the red spheres are oxygen ions); Fig. 2 (b) magnetic structure of $NiFe_2O_4$ (in which the golden spheres are magnetic ions and the red arrows represent the magnitude and the direction magnetic moment of the respective cation).

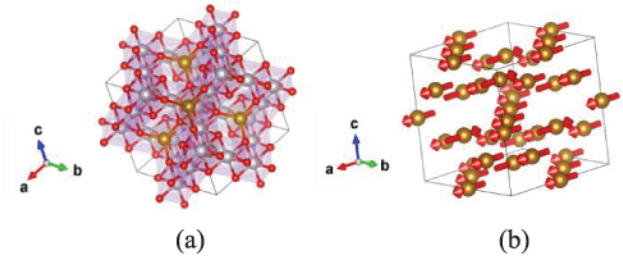

Fig. 2: (a) Structure of $NiFe_2O_4$ super-cell, the golden spheres are tetrahedral (A), purple spheres indicate the octahedral ions (B), the red spheres are oxygen ions, (b) magnetic structure of $NiFe_2O_4$, the golden spheres are magnetic ions and the red arrows represent the magnitude and the direction magnetic moment of the respective cation, both generated by software VESTA [6].

From room temperature of 298K down to 10K, the overall shape diffraction pattern remains the same and no peaks disappear or no extra peaks appear while the temperature was varied, which implies no change in phase occurred as the temperature was lowered. All the neutron diffraction data were analysed by Rietveld refinement method using FullProf software [15]. But for convenience only one set of Rietveld refined pattern taken at 298K temperature have been shown in Fig. 3.

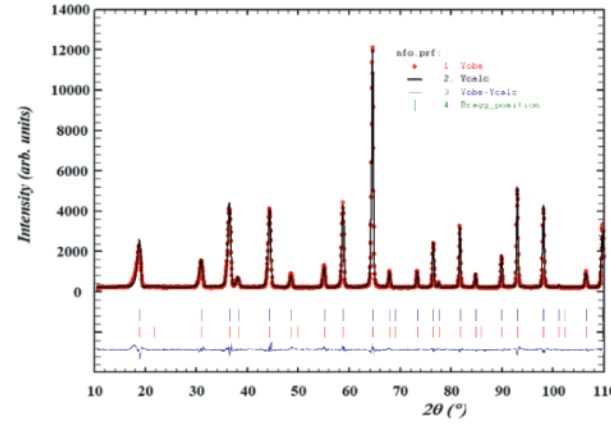

Fig. 3: Rietveld refinement pattern of neutron diffraction data fitted with FullProf software. The red data points are diffraction data, the black line is the calculated pattern, the blue line below is the difference curve, the blue tick mark represents positions of the structural peaks and the red ticks represents the magnetic peaks.

The structural refinement shows the cell parameter (a) is *8.3028*Å at room temperature and as the temperature is reduced the cell parameter reduces to *8.2896* Å at 10K, indicating cell shrinkage. The oxygen anions readjust themselves to accommodate due to shrinkage.

Table 1 shows the reliability factors (R-factors) of the Rietveld refinement using FullProf software for nickel ferrite sample at different temperatures.When temperature of the samples gets reduced, cell vibration gets reduced accordingly. As a result of less vibration, cell parameter also shrinks. To accommodate the shrinkage, oxygen repositions themselves.The variation of lattice parameter 'a' and oxygen position parameter with temperature using best fitting is shown in Fig. 4.

Table 1: Reliability factors (R-factors) of the Rietveld refinement using FullProf software for nickel ferrite sampleat different temperatures

R- factors	10K	50K	100K	200K	298K
R_{Bragg} (%)	2.31	2.43	2.33	2.41	2.77
R_F	1.72	1.79	1.72	1.77	2.11
R_P	10.0	9.86	9.66	10.7	9.87
R_{WP}	11.6	11.4	11.2	12.2	10.3
R_{exp}	6.42	6.42	6.44	6.44	6.90
R_{mag}	5.23	5.55	5.31	5.15	4.60
χ^2	3.253	3.16	3.03	3.588	2.214

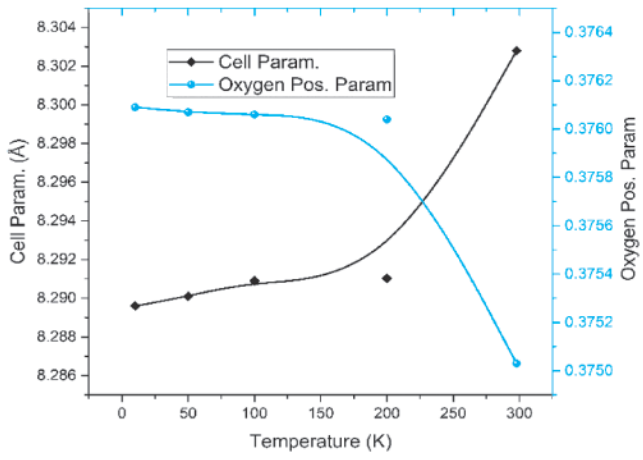

Fig. 4: Variation of cell (lattice) parameter 'a' and oxygen position parameter 'u' with temperature

The magnetic properties of the cations are due to the unfilled inner 3d shell, having the outer shells filled. The spin moment arises from these uncoupled electrons. Also the ratio of the crystal spacing to the unfilled inner shells must be greater than 3.FullProf refinement of neutron diffraction data reveals that the cations concerned are ferro-magnetic, i.e.agree with the above mentioned condition and have magnetic moments (Fe^{2+}, Fe^{3+} and Ni^{2+}). The interaction between A and B sub-lattices are magnetically antiparallel and may have different magnetic moments, thus the material is ferri-magnetic [16].The structural parameters of nickel ferrite sample at different temperaturesis shown in Table 2.

Table 2: The structural parameters of nickel ferrite at different temperatures

Temp. (K)	Cation distribution		Cell parameter a (Å)	Oxygen position parameter O	Overall isotropic displacement factor $B_{overall}$ ($Å^2$)
	Tetrahedral (8a)	Octahedral (16d)			
10	-	-	8.2896	0.37609	0.46365
50	$(Fe^{2})^{+}$	$[Ni^{2+}Fe^{3+}]$	8.2901	0.37607	0.47046
100	-	-	8.2909	0.37606	0.51310
200	-	-	8.2910	0.37604	0.50215
298	-	-	8.3028	0.37503	0.63967

Table 3 shows the tetrahedral and octahedral bond lengths (Δ_{AL}, Δ_{BL}), tetrahedral edge (Δ_{AE}), shared and unshared octahedral edges (Δ_{BE}, Δ_{BEU}); and variation of bond lengths Δ_{AL}(tetrahedral),Δ_{BL}(octahedral) with temperature is shown in Fig. 5.

Table 3: Tetrahedral and octahedral bond lengths (Δ_{AL}, Δ_{BL}), tetrahedral edge (Δ_{AE}), shared and unshared octahedral edges (Δ_{BE}, Δ_{BEU})

Temp. (K)	Δ_{AL} (Å)	Δ_{BL} (Å)	Δ_{AE} (Å)	Δ_{BE} (Å)	Δ_{BEU} (Å)
10	1.8852	2.0264	3.0785	2.7925	2.9372
50	1.8820	2.0235	3.0733	2.7887	2.933
100	1.8821	2.0237	3.0734	2.7892	2.9330
200	1.8818	2.0239	3.0730	2.7897	2.9330
298	1.8699	2.0348	3.0535	2.8175	2.9367

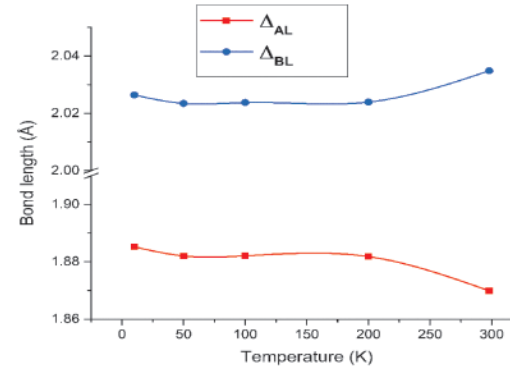

Fig. 5: Variation of bond lengths Δ_{AL}(tetrahedral),Δ_{BL}(octahedral) with temperature

Table 4: The interaction angles θ_1, θ_2, θ_3, θ_4 and θ_5 are given below

θ_1 (°)	θ_2 (°)	θ_3 (°)	θ_4 (°)	θ_5 (°)
123.3114	144.8197	92.8981	125.9279	74.40307
123.3178	144.8479	92.88822	125.9257	74.42031
123.3209	144.862	92.88328	125.9246	74.42893
123.3273	144.8903	92.8734	125.9224	74.44618
123.6503	146.3532	92.37532	125.8111	75.33024

The effective radii of the tetrahedral and octahedral sites were calculated using the following formulae-

$$r_A = C(Fe_A^{+2}) \cdot r(Fe_A^{+2}) \quad (1)$$

$$r_B = \frac{1}{2}[C(Ni_B^{+2}) \cdot r(Ni_B^{+2}) + C(Fe_B^{+3}) \cdot r(Fe_B^{+3})] \quad (2)$$

Here C (M^{n+}) is the concentration of the cation and r (M^{n+}) is the crystal radii of that particular cation. For bivalent Nickel cations the effective crystal radius for six coordination used was 0.83Å (as they are at the octahedral side), for bivalent Fe^{2+} having four coordination 0.77Å and for Fe^{3+} 0.69Å [17].

The position of the O^{2-} anion in the face centered cubic (fcc) lattice is referred to as a quantity called Oxygen position parameter or also anion parameter, u. For ideal spinel structures u_{ideal} is 0.375. To create room for

substituted positive ions, the oxygen ions relocate themselves which gives rise to change in oxygen position parameter.

The relation between effective radii r_A, r_B and r_O^{-2} are as follows, which can be further exploited to calculate the value of *u*.

$$r_{A(Tet)} = \left(u - \frac{1}{4}\right) a\sqrt{3} - r_{O^{-2}} \quad (3)$$

$$r_{B(Oct)} = \left(\frac{5}{8} - u\right) a - r_{O^{-2}} \quad (4)$$

Evidently, the value of *u* is larger than that of ideal spinel structure is due to the replacement of Fe^{3+} with larger Ni^{2+}.

The values of the tetrahedral and octahedral bond lengths (Δ_A and Δ_{BL}), tetrahedral edge (Δ_{AE}) and shared and unshared bond lengths (Δ_{BE} and Δ_{UBE}) can be given by the formulae below [18].

$$\Delta_{AL} = a\sqrt{3}(u - \frac{1}{4}) \quad (5)$$

$$\Delta_{BL} = a\left[(3u^2 - \left(\frac{11}{4}\right)u + \frac{43}{64}\right]^{1/2} \quad (6)$$

$$\Delta_{AE} = a\sqrt{2}\left(2u - \frac{1}{2}\right) \quad (7)$$

$$\Delta_{BE} = a\sqrt{2}\,(1 - 2u) \quad (8)$$

$$\Delta_{BEU} = a\left[4u^2 - 3u + \frac{11}{16}\right]^{\frac{1}{2}} \quad (9)$$

From the calculated values of various bond lengths and interaction angles, it can be seen that Δ_{AL}, Δ_{AE} decreases which is indicative of weakening B-B interaction. On the other hand,Δ_{BL}, Δ_{BE} increases, which is indicating stronger A-A, A-B interaction. The angles are distorted to accommodate the larger Ni^{2+} ions and further when the temperature decreases the angles are further distorted. The angles θ_1, θ_2 indicative of B-B interaction increases, θ_3, θ_4 decreases due to stronger A-B interaction [19, 20].

The magnetic moment of an atom having semi filled inner orbital with uncoupled electron(s) is defined by the equation, $\mu_{s,L} = g\sqrt{\{l(l+1) + 4s(s+1)\}}\mu_B$. Where μ_B is the Bohr magenton, *g* is the Landé splitting factor, S and L are the spin and orbital quantum number. For pure spin moment g=2 and spin quantum number associated with electron spin is ±1/2 [21].

Fe^{3+} ions with octahedral coordination have d^5 high spin (t_{2g}^3 e_g^2) electronic configuration.Theoretically, they must have 5.91μ_B magnetic moment though experimental values vary from 4.9μ_B upto 6.1μ_B. Similarly, Fe^{2+} at tetrahedral coordination have d^6 (e^3 t_2^3) configuration having theoretical moment of 4.9μ_B practically which can be up to 5.5μ_B. The Ni^{2+} ions which have $d^8(t_{2g}^6\ e_g^2)$ configuration have magnetic moment ranging from 2.8μ_B to 3.5μ_B though theoretically they have a moment of 2.83μ_B [22]. The magnetic moments of A and B site cations per unit formula of $NiFe_2O_4$ are presented in table 5.

Table 5: The magnetic moments of site A, site B and net magnetic moment

Temp. (K)	Site A(μ_B) (per unit formula)	Site B (μ_B) (per unit formula)	Net magnetic moment (μ_B)
10	-4.79421	7.65875	2.86454
50	-4.4847	7.15367	2.66897
100	-4.2604	6.668655	2.408255
200	-3.9782	6.2552	2.277
298	-3.4805	5.5468	2.0663

As the temperature is decreased the magnetic moment of A and B site cations increased gradually, but as they have an anti-parallel orientation, the effect of the increasing moment is mostly minimized. The magnetic moments of A and B site cations per unit formula (presented in table 5) and the values agree with the previously studied values of the magnetic moment of bulk Nickel Ferrites [23]. The negative sign indicates the opposite direction of moments compared to B site atoms. A 38% increase of net magnetic moment from 2.0663μ_B to 2.86454μ_B was seen while decreasing temperature from 298K down to 10K which is still substantially low from the theoretically calculated value of net moment [M_A~M_B= (5.9+2.8)-4.9 = 3.78μ_B]. The magnetic moments of site-A, site-B and the net magnetic moment of a unit cell of $NiFe_2O_4$ as temperature varies from 10K to 298K calculated from Rietveld refinement are shown in Fig. 6.

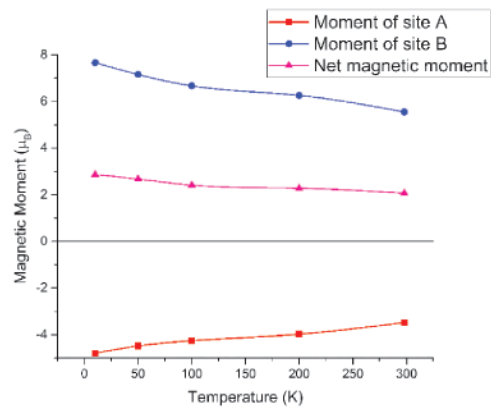

Fig. 6: The magnetic moments of site-A, site-B and the net magnetic moment of a unit cell of $NiFe_2O_4$ as the temperature varies from 10K to 298K calculated from Rietveld refinement

4. Conclusion

The $NiFe_2O_4$ spinel crystal sample was synthesized via PVA evaporation method. The atomic structure, magnetic structure and structural parameters as well as the magnetic moments were measured from the neutron diffraction data through Rietveld analysis. The successive neutron diffraction experiments were performed by gradually

reducing the temperature to 10K. Then the structural and magnetic properties were measured from the analysis of the diffraction data. The $NiFe_2O_4$ sample retained its structural symmetry all along, no phase transitions were observed, though the overall structure suffered from volumetric as well as structural shrinkage. Though the individual magnetic moments of site A and site B were increasing, the net magnetic moment did not change much as the orientations of the magnetic moments are anti-parallel and thus balanced the increment. The net moment increased from $2.0663\mu_B$ to $2.86454\mu_B$ as there is twice the number of cations in B site compared to A sites.

Acknowledgements

The authors are thankful to the Center for Research Reactor (CRR) of Bangladesh Atomic Energy Commission for sample irradiation to perform the nettron diffraction studies. The technical staff of neutron scattering group of RNPD are gratefully acknowledged for their help during sample preparation and the nettron diffraction experiments.

References

1. R. Valenzuela, Novel applications of ferrites, Phys. Res. Int., **2012(Special Issue)**, 591839 (2012).
2. D.H.K. Reddy and Y.S. Yun, Spinel ferrite magnetic adsorbents: Alternative future materials for water purification?, Coord. Chem. Rev., **315**, 90-111 (2016).
3. M. Nogues, G. Villers, J.L. Dormann and J. Teillet, High Field Magnetization in Randomly Canted Ferrites, IEEE Trans. Magn., (1990).
4. J. Rodríguez, Carvajal, Recent advances in magnetic structure determination by neutron powder diffraction, Phys. B Phys. Condens. Matter, **192(1-2)**, 55-69 (1993).
5. S.S.A. Allah, A.M. Balagurov, A. Hashhash, I.A. Bobrikov and S. Hamdy, Refinement of atomic and magnetic structures using neutron diffraction for synthesized bulk and nano-nickel zinc gallate ferrite, Phys. B Condens. Matter, **481**, 118-123 (2016).
6. K. Momma and F. Izumi, VESTA 3 for three-dimensional visualization of crystal, volumetric and morphology data, J. Appl. Crystallogr., **44(6)**, 1272-1276 (2011).
7. I.B. Elius, B.M. Asif, J. Maudood, T.K. Datta, A.K. M. Zakaria, S. Hossain, M.S. Aktar and I. Kamal, Synthesis and Characterization of Strontium Doped Barium Titanates using Neutron Diffraction Technique, Nucl. Sci. Appl., **28(1)**, 57-62 (2019).
8. P. Pramanik and A. Pathak, A new chemical route for the preparation of fine ferrite powders, Bull. Mater. Sci., (1994).
9. I. Kamal, S.M. Yunus, T.K. Datta, A.K. M. Zakaria, A.K. Das, S. Aktar, S. Hossain, R. Berliner and W. B. Yelon, A high performance neutron powder diffractometer at 3 MW Triga Mark-II research reactor in Bangladesh, AIP Conf. Proc., (2016).
10. S. Khanam, A.K.M. Zakaria, M.H. Ahsan, T.K. Datta, S. Aktar, S.I. Liba, S. Hossain, A.K. Das, I. Kamal, S.M. Yunus, D.K. Saha and S.G. Eriksson, Study of the Crystallographic and Magnetic Structure in the Nickel Substituted Cobalt Ferrites by Neutron Diffraction, Mater. Sci. Appl., **06(04)**, 332-342 (2015).
11. N. Jahan, A.K.M. Zakaria, F.U. Z. Chowdhury, M.S. Aktar and T.K. Datta, Study of the cation distribution and crystallographic properties of the spinel system $NiCr_xFe_{2-x}O_4$ ($0.0\leq x\leq 1.0$) by neutron diffraction, Mater. Chem. Phys., **202**, 225-233 (2017).
12. J.R. Carvajal, A program for calculating irreducible representation of little groups and basis functions of polar and axial vector properties, .
13. J. Dawidowski, J.R. Granada, J.R. Santisteban, F. Cantargi and L.A.R. Palomino, Neutron Scattering Lengths and Cross Sections, Exp. Methods Phys. Sci., **44(3)**, 471-528 (2013).
14. J.R. Carvajal, ChemInform Abstract: Magnetic Structure Determination from Powder Diffraction Using the Program FullProf, Appl. Crystallogr., **32(51)**, 30-36 (2001).
15. R. Carvajal, Tutorial on Magnetic Structure Determination and Refinement using Neutron Powder Diffraction and FullProf, (2014).
16. I.B. Elius, S. Hossain, S. Akter, S.M. Hoque, I. Kamal and A.K. Azad, Structural and magnetic characterization of $Ni_xCu_{0.8-x}Zn_{0.2}Fe_2O_4$ spinel ferrites, Ferroelectrics, **572**, (2020).
17. R. D. Shannon and C. T. Prewitt, Revised values of effective ionic radii, Acta Crystallogr. Sect. B Struct. Crystallogr. Cryst. Chem., (1970).
18. Z.K. Heiba, M.B. Mohamed, L. Arda and N. Dogan, Cation distribution correlated with magnetic properties of nanocrystalline gadolinium substituted nickel ferrite, J. Magn. Magn. Mater., **391**, 195-202 (2015).
19. Z.K. Heiba, M.B. Mohamed and S.I. Ahmed, Cation distribution correlated with magnetic properties of cobalt ferrite nanoparticles defective by vanadium doping, J. Magn. Magn. Mater., **441**, 409-416 (2017).
20. R.A. Pawar, S.M. Patange, A.R. Shitre, S.K. Gore, S.S. Jadhav and S. E. Shirsath, Crystal chemistry and single-phase synthesis of Gd^{3+} substituted Co-Zn ferrite nanoparticles for enhanced magnetic properties, RSC Adv., **8(44)**, 25258-25267 (2018).
21. G. Rangarajan and M.S. Vijaya, Materials Science, **3rd ed.** Tata McGraw-Hill (2004).
22. K.C. De Berg and K.J. Chapman, Determination of the magnetic moments of transition metal complexes using rare earth magnets, J. Chem. Educ., **78(5)**, 670-673 (2001).
23. R.M. More, T.J. Shinde, N.D. Choudhari and P.N. Vasambekar, Effect of temperature on X-ray, IR and magnetic properties of nickel ferrite prepared by oxalate co-precipitation method, J. Mater. Sci. Mater. Electron., (2005).